Preliminary Measurement of Time-Dependent B_d^0–$\overline{B_d^0}$ Mixing Using Topology and Charge Selected Semi-Leptonic B Decays*

The SLD Collaboration*

Abstract

The time dependence of B_d^0–$\overline{B_d^0}$ mixing has been measured using a sample of 150,000 hadronic Z^0 decays collected by the SLD experiment at the SLC between 1993 and 1995. The analysis identifies the semileptonic decays of B mesons with high (p, p_t) leptons and reconstructs the B meson decay length and charge by vertexing the lepton with a partially reconstructed D meson. Vertex charge is used to enrich the selection of neutral over charged B mesons. This method results in a sample of 581 neutral decays with high charge purity. The B candidate is tagged at production with a combined tag that exploits the large polarized b forward-backward asymmetry in conjunction with the opposite hemisphere b jet charge. The final state is tagged by the sign of the high (p, p_t) lepton. From our preliminary analysis we find a mass difference between the two B_d^0 mass eigenstates of, $\Delta m_d = 0.452 \pm 0.074(stat) \pm 0.049(syst)$ ps^{-1}.

Paper Contributed to the XXVIII International Conference on High Energy Physics, July 25-31, 1996, Warsaw, Poland

1

1 Introduction

B_d^0–$\overline{B_d^0}$ mixing occurs via a second order weak interaction in complete analogy to the mixing observed in the $K^0 - \overline{K^0}$ system. The flavor eigenstates of the B^0 are written in terms of the mass eigenstates B_1 and B_2, as $B^0 = (B_1 + B_2)/\sqrt{2}$ and $\overline{B^0} = (B_1 - B_2)/\sqrt{2}$. Unlike the neutral kaon system the difference between the B meson lifetimes is expected to be small. Hence, the probability that a meson created as a B^0 ($\overline{B^0}$) will decay as a B^0 ($\overline{B^0}$) after proper time t can be written as

$$P_u(t) = \frac{\Gamma}{2} e^{-\Gamma t} \left(1 + \cos \Delta m_d\, t\right) , \tag{1}$$

where Δm_d is the mass difference between the mass eigenstates, Γ is the decay width for both states and P_u denotes the probability to remain 'unmixed'. The effects of CP violation are assumed to be small and are neglected. Similarly, the probability that the same initial state will 'mix' and decay as its antiparticle is

$$P_m(t) = \frac{\Gamma}{2} e^{-\Gamma t} \left(1 - \cos \Delta m_d\, t\right) . \tag{2}$$

This paper presents the current status of a measurement made with the SLD detector of time dependent B_d^0 mixing. The measurement presented here uses a sample of 150,000 hadronic Z^0 decays collected between 1993 and 1995 by the SLD experiment at the SLAC Linear Collider (SLC). The analysis determines the B decay length by intersecting a high (p, p_t) lepton track with a topologically reconstructed D meson. Events are categorized as mixed or unmixed on the basis of flavor tags which determine the particle-antiparticle nature of the B at production (the initial state at t=0) and decay (final state). The initial state is tagged as having originated from a b or a $\bar{b}$ quark using a polarized b asymmetry plus jet charge tag. The polarization tag, unique to the SLD experiment, is a very powerful tag of the initial state. The final state is tagged using the sign of the lepton.

2 Event Selection and Vertexing

The first step in this analysis is to reconstruct the charged track topology of semileptonic B decays. The algorithm reconstructs both B and cascade D vertices. The B vertex contains the lepton and at most one other track, and the D vertex contains two, three or four tracks. This topological technique does not use the charge correlation between the lepton and the D vertex but determines the total charge of the B meson from the sum of charges in the B and D vertices. The final charge assignment purity will be somewhat diluted, however, due to the fraction of decays of the type

$B^+ \to \bar{D}^{**0}l^+\nu$ which can yield two slow transition pions at the B vertex. (Charge conjugation is implied throughout this paper.)

2.1 The SLD Detector

This analysis relies on SLD's calorimetry and tracking systems (detailed descriptions can be found in Ref. [1]). The Liquid Argon Calorimeter (LAC) provides excellent solid-angle coverage ($|\cos\theta| < 0.84$ and $0.82 < |\cos\theta| < 0.98$ in the barrel and end-cap regions, respectively). The Warm Iron Calorimeter (WIC) also covers much of the solid-angle ($|\cos\theta| < 0.95$) and provides maximal muon identification efficiency for $|\cos\theta| < 0.60$. The LAC is divided longitudinally into two sections with energy resolution in the electromagnetic section measured to be $\sigma/E = 15\%/\sqrt{E(GeV)}$, and that in the hadronic section estimated to be $60\%/\sqrt{E(GeV)}$. Tracking is provided by the Central Drift Chamber (CDC) and the CCD pixel Vertex Detector (VXD) with maximal track reconstruction efficiency for $|\cos\theta| < 0.74$. Charged tracks are first reconstructed in the CDC and linked with clusters in the VXD, and then a combined fit is performed. The momentum resolution of the combined fit is $\sigma_{p_\perp}/p_\perp = \sqrt{(0.01)^2 + (0.0026/p_\perp)^2}$, where $p_\perp$ is the track momentum transverse to the beam direction in GeV/c. The impact parameter resolution was measured using the miss distance between the two tracks in $Z^0 \to \mu^+\mu^-$ decays. This yields a high-momentum single-track resolution of 11 μm in the plane perpendicular to the beam direction (xy plane) and 38 μm in the plane containing the beam axis (rz plane).

The position of the micron-sized SLC Interaction Point (IP) in the xy plane is reconstructed with a measured precision of $\sigma_{IP} = (7 \pm 2)$ μm using tracks in sets of ~ 30 sequential hadronic Z^0 decays. The z position of the Z^0 primary vertex is determined on an event-by-event basis using the median z position of tracks at their point-of-closest-approach to the IP in the xy plane. The simulation described below estimates a precision of ~ 52 μm in this quantity for $Z^0 \to b\bar{b}$ decays [1].

2.2 Detector Simulation

The mixing measurement relies on a Monte Carlo simulation based on the JETSET 7.4 event generator[2] and the GEANT 3.21 detector simulation package[3]. The b-quark fragmentation followed the Peterson *et al.* parametrization[4]. B mesons were generated with mean lifetime $\tau = 1.55$ ps and B baryons with $\tau = 1.10$ ps. B hadron decays were modelled according to the CLEO B decay model [5] tuned to reproduce the spectra and multiplicities of leptons, charmed hadrons, pions, kaons, and protons, measured at the $\Upsilon(4S)$ by ARGUS and CLEO [6]-[7]. B baryon and charmed hadron decays were modelled using JETSET with, in the latter case,

branching fractions tuned to existing measurements[15].

2.3   Lepton Identification

Electron candidates are required to have a measured energy in the LAC which agrees
with the momentum of the associated track measured in the CDC, to have little or
no LAC hadronic energy, and to have a front/back electromagnetic energy ratio
consistent with that expected for electrons[9]. Muon candidates are required to
have a good match between hits found in the WIC and tracks extrapolated from
the CDC, taking into account track extrapolation errors and multiple scattering[9].
To enhance the fraction of $Z^0 \rightarrow b\,\bar{b}$ events with relatively small loss in efficiency,
lepton candidates are required to pass relatively loose cuts: total momentum $p > 2$
GeV/c and momentum transverse to the nearest jet $p_t > 0.4$ GeV/c (where jets are
found from calorimeter clusters using the JADE algorithm [10] with $y_{cut} = 0.005$).
Application of these cuts yields a sample of 34K events, including approximately
75% of the electrons and muons from semileptonic B decays within $|\cos\theta| < 0.6$.

2.4   Vertex Reconstruction

The B and D decay vertex reconstruction proceeds separately for each event hemi-
sphere containing a lepton using a multi-pass algorithm which operates on those
tracks which have at least one VXD hit and are classified as either primary or sec-
ondary. The first step of this track classification scheme is to remove tracks from
identified γ conversions, or from identified K^0 or Λ decays. The remaining tracks are
classified as primary unless their 3-D impact parameter with respect to the primary
vertex $> 3.5\sigma$ and their momentum $p > 0.8$ GeV/c, in which case they are classified
as secondary.

In the first pass, the event hemisphere containing the lepton candidate is required
to contain no more than four secondary tracks (excluding the lepton) and a D vertex
is constructed using all such tracks (vertex cuts are defined below). The D trajectory,
found from the D vertex and the total momentum vector of tracks included in the
vertex, must intersect the lepton to form a valid (one-prong) B vertex solution.
If this step is successful, an attempt is made to form a two-prong B vertex by
attaching one primary track to the lepton near the point of intersection. This first
pass identifies 91% of the final candidates. In the second pass, the first pass successes
are allowed to be modified by searching for primary tracks which can be added to the
existing D vertex. This search is successful for 40% of the initial pass 1 candidates
and they are reclassified as pass 2. Multiple solutions are sorted on the basis of the
smallest impact parameter between the D trajectory and the lepton or B vertex.
The third pass is performed on those hemispheres in which no pass 1 candidate was
identified. In this pass, a search is made for solutions in which one secondary track

	B Vertex	D Vertex		Data	MC
	1 prong	2 prong	519	$(38.0 \pm 1.3)\%$	33.7%
B^+	1 prong	4 prong	115	$(8.4 \pm 0.8)\%$	10.1%
	2 prong	3 prong	149	$(10.9 \pm 0.8)\%$	10.0%
	1 prong	3 prong	341	$(24.9 \pm 1.2)\%$	28.7%
B^0	2 prong	2 prong	175	$(12.8 \pm 0.9)\%$	12.7%
	2 prong	4 prong	68	$(5.0 \pm 0.6)\%$	4.8%

Table 1: Summary of reconstructed topologies, including the fraction of the total number of semileptonic B decay candidates for data and Monte Carlo simulation.

makes a valid B vertex with the lepton, the remaining secondary tracks form a D vertex, and the D trajectory intersects the B vertex. This third pass identifies the remaining 9% of the final candidates. In all passes, at most one track is added to the lepton to form the B vertex and at most two tracks are added to the original D vertex.

The requirements for tracks to form a D vertex are: the absolute value of the charge ≤ 1, the mass (charged tracks assumed to be π's) < 1.98 GeV, the vertex displacement from the IP $> 4\ \sigma$ and < 2.5 cm, and the vertex χ^2 (2,3,4 prongs) $< (4, 12, 20)$. The requirements for tracks to form a B vertex are: the absolute value of the total charge $(B + D) \leq 1$, the mass $(B + D$ tracks$) > 1.4$ GeV, the observed decay length (displacement from IP) > 0.08 cm and < 2.4 cm, and the momentum of the non-lepton track (if any) > 0.4 GeV/c. The requirements for the D vertex to be linked to the B vertex are: the distance between D and B vertices $> 200\ \mu$m, and for one-prong B, the distance of closest approach of the D vector with the lepton, $< (130, 100, 70)\ \mu$m for (2, 3, 4) prong D vertices, while for two-prong B, the three-dimensional impact parameter of the D vector with respect to the B vertex $< 200\ \mu$m.

The analysis described above isolates 1367 semileptonic B decay candidates. Of these, 783 are reconstructed as charged decays and 584 as neutral decays, with the topological breakdown given in Table 1 together with predictions from the simulation. Only the neutral decays are used in this analysis. A few candidates are lost due to a lack of a polarization measurement, bringing the total number of neutral candidates used in the fits to 581. Using the Monte Carlo simulation, the efficiency for reconstructing a semileptonic B decay is estimated to be 24% for decays with an identified lepton within $|\cos\theta| < 0.6$.

Monte Carlo studies show that neutral sample is 99.1% pure in B hadrons. The simulated flavor contents are 19.6% B_u^+, 60.8% B_d^0, 14.0% B_s^0, and 4.7% B baryons for the neutral sample. The rate of lepton mis-tagging (wrong sign leptons) is 15% for charge zero vertices, as determined from our simulation.

Checks of the charge assignment algorithm have been performed and are detailed in Ref. [12].

3 Flavor Tagging

In the second part of this analysis the candidate events are categorized as mixed or unmixed. In order to do this, it is necessary to determine the B or $\bar{B}$ nature of the candidate at both production (initial state, t=0) and decay (final state). The initial state flavor tagging takes advantage of the large polarized forward-backward asymmetry for $Z^0 \to b\bar{b}$ decays and also uses a jet charge technique. The final state flavor tag uses the sign of the high p_t lepton.

The large forward-backward asymmetry for $Z^0 \to b\bar{b}$ decays is used as an efficient tag of the initial state flavor. The effective analyzing power for the polarization tag is given by the forward-backward asymmetry in Z production,

$$A_{pol} = 2A_b \, \frac{A_e + \mathcal{P}_e}{1 + A_e \mathcal{P}_e} \, \frac{cos\theta_T}{1 + cos^2\theta_T} \, , \tag{3}$$

where $A_b = 0.94$, $A_e = 0.155$, $\mathcal{P}_e$ is the electron beam longitudinal polarization, and θ_T is the angle between the thrust axis and the electron beam direction (the thrust axis is signed such that it points in the same hemisphere as the reconstructed vertex). This yields a correct tag probability of 76% (62%) for an average electron polarization $\mathcal{P}_e = 77\%$ (63%). The correct tag probability is expressed as

$$P_{pol} = \frac{1}{2}(1 + A_{pol}) \, . \tag{4}$$

The separation of events originating from b vs. $\bar{b}$ quarks is shown in Fig. 1a.

A jet charge technique is also used in addition to the polarized forward-backward asymmetry. For this tag, tracks in the hemisphere opposite that of the reconstructed vertex are selected. These tracks are required to have momentum transverse to the beam axis $p_\perp > 0.15$ GeV/c, total momentum $p < 50$ GeV/c, impact parameter in the plane perpendicular to the beam axis $\delta < 2$ cm, distance between the primary vertex and the track at the point of closest approach along the beam axis $\Delta z < 10$ cm, and $|cos\theta| < 0.8$. With these tracks, an opposite hemisphere momentum-weighted track charge is defined as

$$Q_{jet} = \sum_i q_i \left| \vec{p}_i \cdot \hat{T} \right|^\kappa \, , \tag{5}$$

where q_i is the electric charge of track i, $\vec{p}_i$ its momentum vector, $\hat{T}$ is the thrust axis direction, and κ is a coefficient chosen to be 0.5 to maximize the separation between
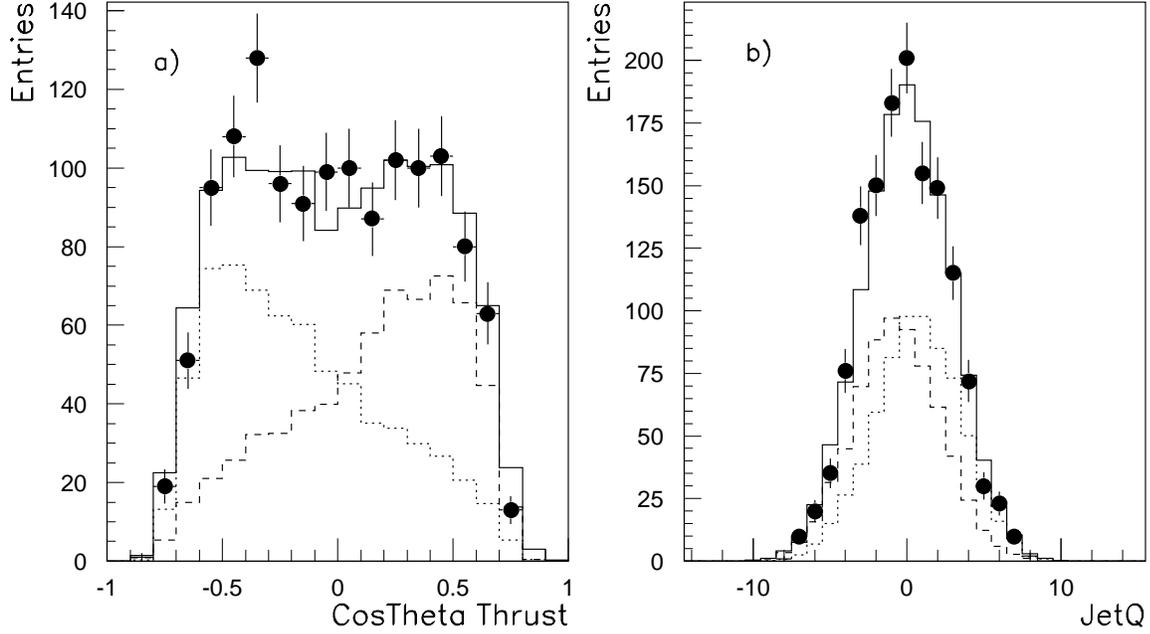
Figure 1: Initial state tag variables for data (points) and MC (solid line) with MC b and $\overline{b}$ quark components (dashed and dotted lines respectively).

b and $\overline{b}$ quarks. The separation is shown in Fig. 1b. The probability for correctly tagging an initial state b quark in the vertex hemisphere can be parameterized as

$$P_{jet} = \frac{1}{1 + e^{\alpha Q_{jet}}} \; , \tag{6}$$

where the coefficient $\alpha = -0.26$ as determined using the Monte Carlo simulation. This technique yields an overall correct tag probability of 68% and is essentially independent of the polarized forward-backward asymmetry tag.

The two initial state tags can be combined to form an overall initial state tag. The correct sign probability for the combined tag can be written as

$$P_i = \frac{P_{pol} P_{jet}}{P_{pol} P_{jet} + (1 - P_{pol})(1 - P_{jet})} \; . \tag{7}$$

The combination of the two tags yields an overall correct tag probability of 80%.

The sign of the high P_t lepton in the final state tags the B at decay with high probability. The correct tag probability as determined from the Monte Carlo is 85%.

4 B_d^0–$\overline{B_d^0}$ Mixing Measurement

The initial state tag probability P_i (Eq. 7) and the probability of the final state tag P_f each have an analyzing power $a_{i,f} = |2P_{i,f} - 1|$. The probability of mixing, that is a B_d^0 vertex produced by a decaying b ($\overline{b}$) quark that originated as a $\overline{b}$ (b) quark is

$$P_M = P_i(b)P_f(\overline{b}) + P_i(\overline{b})P_f(b) \qquad (8)$$

with overall tag analyzing power $a_t = a_i a_f$. The B_d^0 time dependent mixing parameter is extracted using a χ^2 fit of the data mixed fraction to the Monte Carlo in bins of reconstructed decay length. The mixed fraction in each bin is the number of events tagged as mixed ($P_M > 0.5$) divided by the total. Each entry is weighted by a_t to optimize the tag information.

The χ^2 fit is made to the MC for a range of Δm_d values by generating MC mixed fraction distributions for arbitrary Δm_d in the following way. The MC B_d^0 mixing is 'switched off' by reversing the sign of the final state tag if the vertex is a B_d^0 decay resulting from a $b/\overline{b}$ quark which had mixed at the MC truth level. From this $\Delta m_d = 0.0$ MC distributions are generated labeled M_0 and U_0 for vertices tagged as mixed ($P_M > 0.5$) and unmixed ($P_M < 0.5$) respectively with entries weighted by a_t. Corresponding distributions for arbitrary Δm_d, labeled $M_{\Delta m_d}$ and $U_{\Delta m_d}$, are then generated by combining the entries in M_0 and U_0 using a further weight W:

$$W = \frac{1}{2}(1 + \cos(\Delta m_d t)) , \qquad (9)$$

which is the probability that a b quark remains a b quark given the mixing parameter Δm_d and a B_d^0 meson decaying after the MC proper time t. The weight is calculated and applied to each entry in the original histograms as indicated below

$$M_{\Delta m_d} = W M_0 + (1 - W)U_0 ,$$

$$U_{\Delta m_d} = W U_0 + (1 - W)M_0 .$$

The MC mixed fraction $\frac{M_{\Delta m_d}}{M_{\Delta m_d} + U_{\Delta m_d}}$ follows trivially and the χ^2 of the data fit to the MC is determined as a function of the MC Δm_d in order to derive the B_d^0 mixing parameter in the data.

The unmixed and mixed decay length distributions for the neutral vertex selected sample are shown in Fig. 2(a,b). The mixed fraction as a function of decay length is shown in Fig. 2(c). Superimposed on this figure is the best Monte Carlo fit to the data, as well as the Monte Carlo prediction when mixing is turned off. The data shows a significant deviation from the no mixing result. In Fig. 2(d) the results of
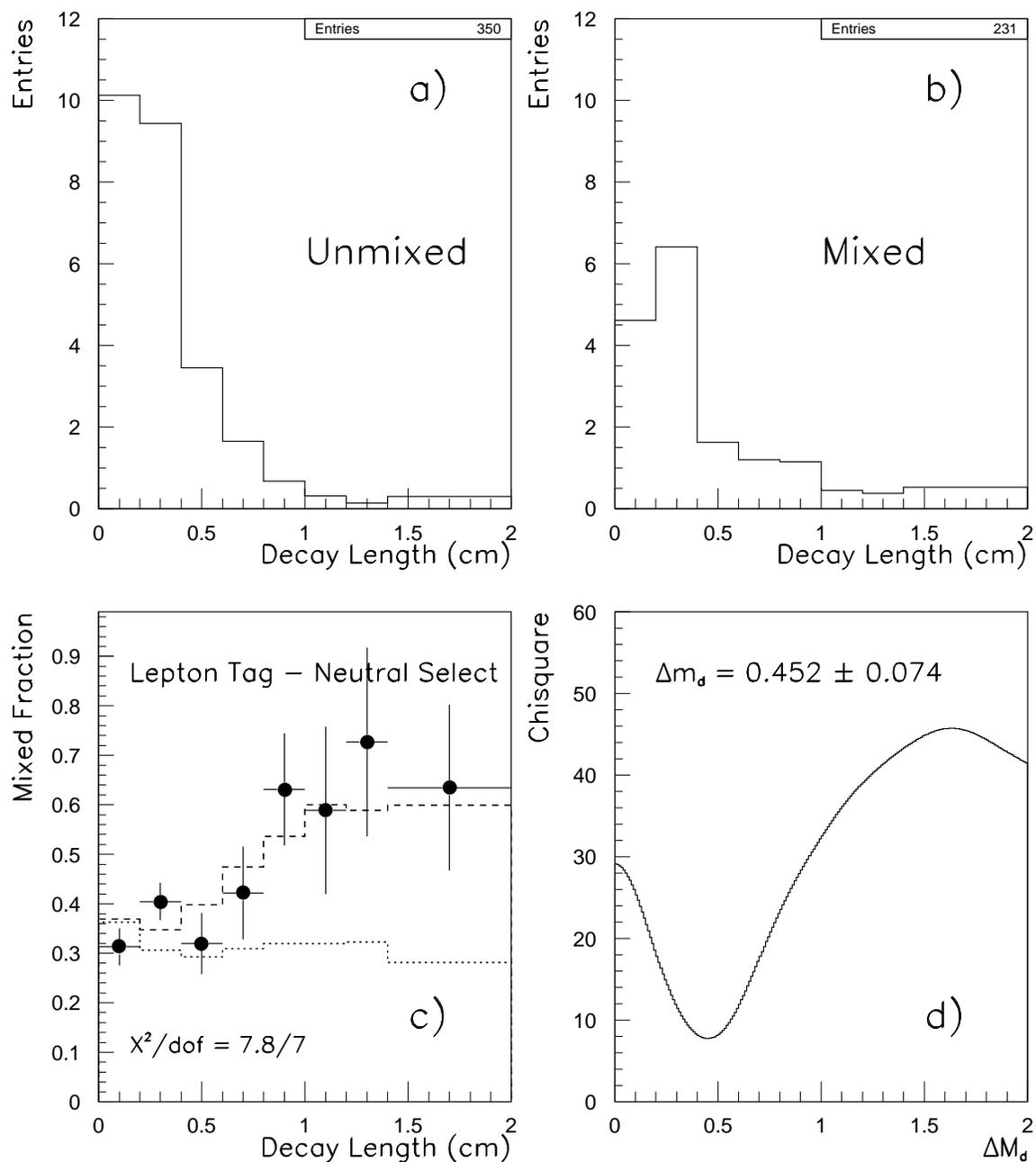
SLD-Preliminary: Neutral B Vertex

Figure 2: Fraction of mixed decays as a function of decay length for the lepton tag analysis. Shown are data (points), best fit MC (dashed histograms) and MC without B_d^0 mixing (dotted histograms).

the chi-square fit are shown as a function of the mixing parameter. The fit finds a minimum at $\Delta m_d = 0.452 \pm 0.074$.
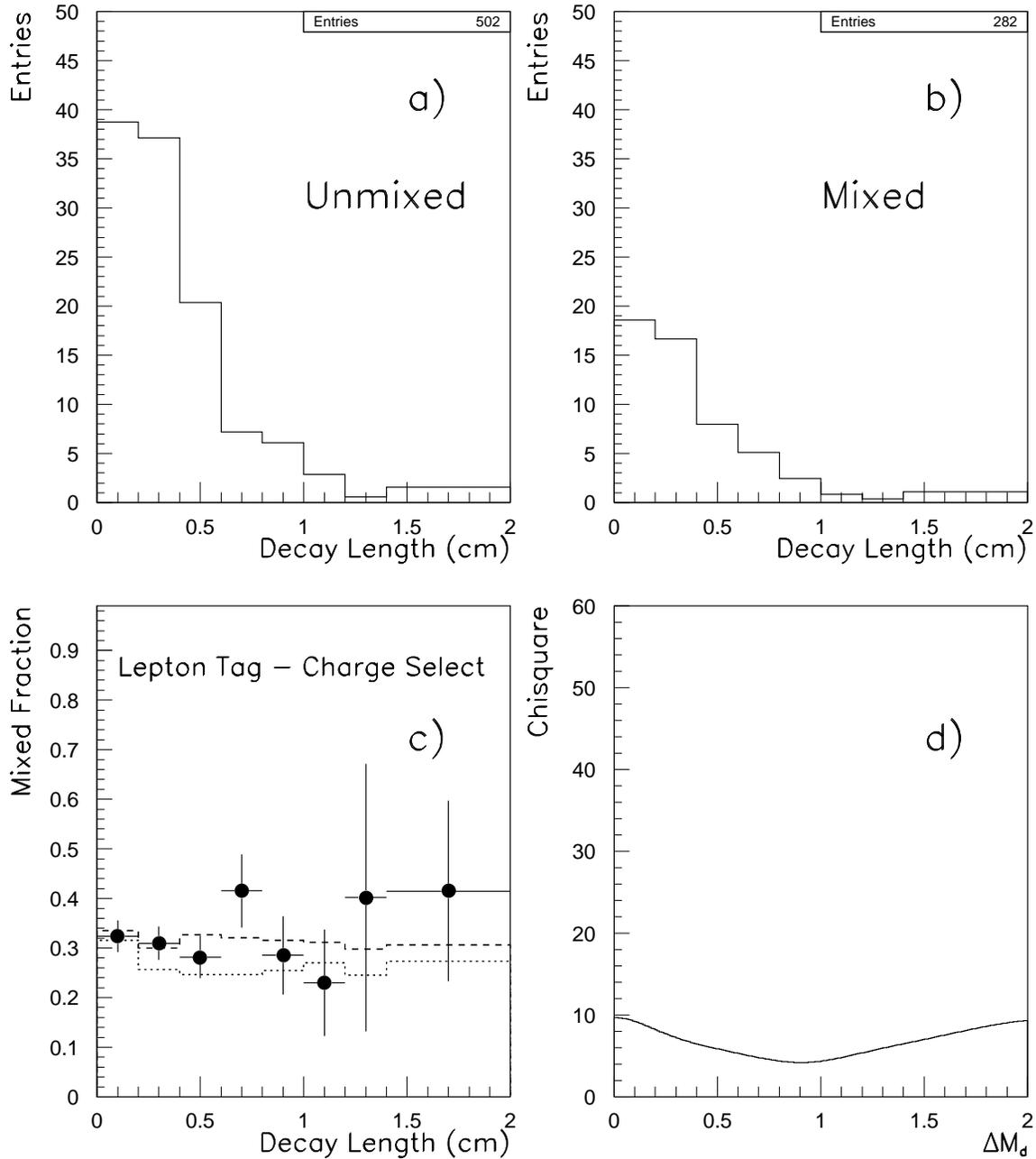
Figure 3: Fraction of mixed decays as a function of decay length for the lepton tag analysis when charged vertices are selected. As expected, the mixing signal vanishes.

It is interesting also to see what result is obtained if one chooses the charged vertex sample rather than the neutral vertex sample. In Fig. 3 we display the results of the analysis performed on the charged vertex sample. As one would expect from a sample dominated by $B^{\pm}$, the mixing signal vanishes.

5   Systematic Uncertainties

The total systematic error extracted below includes effects due to the uncertainty in the detector and physics modeling, and in the fitting technique. The results are summarized in Table 2.

The systematic contribution due to uncertainties in detector modeling include tracking efficiency, detector resolution, and lepton identification. A discrepancy in the average number of tracks was observed comparing data and Monte Carlo simulation. This was corrected for in the simulation by removing the appropriate number of tracks, taking into account the dependence of the effect on track p_T, $\cos \theta$, azimuthal angle and angle between the track and the nearest jet axis. On average, 3.8% of the tracks used in this analysis were removed from the simulation. We assigned as a systematic uncertainty the entire difference between fit results obtained with and without this track efficiency correction. Detailed checks of the track resolution modeling were also performed. It was found that the simulation reproduces the distribution of the track impact parameter in the $r\phi$ plane very well, but appeared to be somewhat narrower than the data in the core of the impact parameter distribution in the rz plane. This is attributed to residual misalignments within the VXD. A correction was applied to account for this and the quoted systematic uncertainty corresponds to the difference between results obtained with and without this correction.

We have studied the sensitivity of the measurement to the production characteristics of B hadrons in Z decays, as well as to the B and D decay models. The uncertainty in the fragmentation of the b-quark was studied by varying the value of ϵ in the Peterson *et al.* fragmentation parametrization, such as to modify the mean fractional energy of B hadrons according to $\langle x_E \rangle = 0.700 \pm 0.011[13]$. The dependence on the shape of the $\langle x_E \rangle$ distribution was also included in the total fragmentation uncertainty[14].

The sensitivity to the B decay model was investigated by varying branching ratios, track multiplicities and lifetimes.

The sensitivity of the result to the fit range and binning was investigated by repeating the fit for a number of different binnings and decay length ranges.

6   Summary

From our preliminary analysis we find a mass difference between the two B_d^0 mass eigenstates of, $\Delta m_d = 0.452 \pm 0.074(stat) \pm 0.049(syst)$ ps^{-1}.

Tracking efficiency	0.017	Track Eff. Corr. On/Off
Detector resolution	0.010	VXD z-correction On/Off
Lepton mis-ID	0.003	$\pm 10\%$
b fragmentation	0.009	$\langle x_E \rangle = 0.700 \pm .011$ & shape
B_d lifetime	0.004	1.55 ± 0.10 ps
B_s lifetime	0.009	1.55 ± 0.15 ps
B baryon lifetime	0.003	1.10 ± 0.11 ps
B_s fraction in $b\bar{b}$	0.004	$(11.5 \pm 4)\%$
B baryon fraction in $b\bar{b}$	0.002	$(7.2 \pm 4)\%$
B_s mixing	0.009	$\Delta m_s = [5, \infty]\text{ps}^{-1}$
$b \to c \to l$	0.003	$(9.3 \pm 0.5)\%$
B.R.$(B_d \to c \to l/b \to c \to l)$	0.003	$(40.7 \pm 4)\%$
B.R.$(B \to D^{**}l\nu/B \to l\nu X)$	0.007	$(23.2 \pm 11)\%$
B.R.$(B \to DDX)$	0.002	$(15 \pm 5)\%$
Charm lifetime	0.004	$D^0, D^\pm, D_s, \Lambda_c$
Tagging parameters	0.011	$P_e \pm 1.0\%$, $A_b \pm 0.04\%$, $\alpha \pm 10\%$
Fit Systematics	0.032	Decay Length binning & range
MC Statistics	0.021	
Total	0.049	

Table 2: Summary of contributions to the systematic uncertainty in Δm_d for the lepton tag analysis.

References

[1] K. Abe *et al.*, Phys. Rev. **D53**, 1023 (1996).

[2] T. Sjöstrand, CERN-TH-7112-93, Feb. 1994.

[3] R. Brun *et al.*, CERN-DD/EE/84-1, 1989.

[4] C. Peterson *et al.*, Phys. Rev. **D27**, 105 (1983).

[5] CLEO QQ MC code provided by P. Kim and the CLEO Collaboration.

[6] CLEO Collaboration: B. Barish *et. al.*, **CLNS-95-1362** (1995);
ARGUS Collaboration: H. Albrecht *et. al.*, *Z. Phys.* **C58**, 191 (1993);
ARGUS Collaboration: H. Albrecht *et. al.*, *Z. Phys.* **C62**, 371 (1994);
F. Muheim (CLEO Collaboration), talk presented at the 8th DPF Meeting, Albuquerque, New Mexico, Aug 1994;

M. Thulasidas, Ph.D thesis, Syracuse University (1993);
CLEO Collaboration: G. Crawford *et. al.*, *Phys. Rev.* **D45**, 752 (1992)
CLEO Collaboration: D. Bortoletto *et. al.*, *Phys. Rev.* **D45**, 21 (1992).

[7] T.R. Junk, Ph.D. Thesis, Stanford University, SLAC-Report-95-476, Nov. 1995.

[8] Particle Data Group, Phys. Rev. **D50**, Part I (1994).

[9] K. Abe *et al.*, Phys. Rev. Lett. **74**, 2895 (1995).

[10] S. Bethke *et al.*, Phys. Lett. **213B**, 235 (1988).

[11] H.Albrecht *et al.*, Z. Phys. **C62**, 371 (1994).

[12] See the SLD semi-leptonic B lifetime measurement contributed to this conference, ICHEP-96 PA05-084.

[13] see for example,
R. Akers *et al.*, Z. Phys. **C60**, 199 (1993);
D. Buskulic *et al.*, Z. Phys. **C62**, 179 (1994);
P. Abreu *et al.*, Z. Phys. **C66**, 323 (1995).

[14] M. G. Bowler, Z. Phys. **C11**, 169 (1981).

[15] Particle Data Group, Phys. Rev. **D50**, Part I (1994).

[16] H.Albrecht *et al.*, Z. Phys. **C54**, 13 (1992);
R.Giles *et al.*, Phys. Rev. **D30**, 2279 (1984).

[17] D.Coffman *et al.*, Phys. Lett. **B263**, 135 (1991);

*List of Authors

K. Abe,[19] K. Abe,[29] I. Abt,[13] T. Akagi,[27] N.J. Allen,[4] W.W. Ash,[27]†
D. Aston,[27] K.G. Baird,[24] C. Baltay,[33] H.R. Band,[32] M.B. Barakat,[33]
G. Baranko,[9] O. Bardon,[15] T. Barklow,[27] A.O. Bazarko,[10] R. Ben-David,[33]
A.C. Benvenuti,[2] G.M. Bilei,[22] D. Bisello,[21] G. Blaylock,[6] J.R. Bogart,[27]
B. Bolen,[17] T. Bolton,[10] G.R. Bower,[27] J.E. Brau,[20] M. Breidenbach,[27]
W.M. Bugg,[28] D. Burke,[27] T.H. Burnett,[31] P.N. Burrows,[15] W. Busza,[15]
A. Calcaterra,[12] D.O. Caldwell,[5] D. Calloway,[27] B. Camanzi,[11]
M. Carpinelli,[23] R. Cassell,[27] R. Castaldi,[23](a) A. Castro,[21]
M. Cavalli-Sforza,[6] A. Chou,[27] E. Church,[31] H.O. Cohn,[28] J.A. Coller,[3]
V. Cook,[31] R. Cotton,[4] R.F. Cowan,[15] D.G. Coyne,[6] G. Crawford,[27]
A. D'Oliveira,[7] C.J.S. Damerell,[25] M. Daoudi,[27] R. De Sangro,[12]
R. Dell'Orso,[23] P.J. Dervan,[4] M. Dima,[8] D.N. Dong,[15] P.Y.C. Du,[28]
R. Dubois,[27] B.I. Eisenstein,[13] R. Elia,[27] E. Etzion,[4] D. Falciai,[22] C. Fan,[9]

M.J. Fero,[15] R. Frey,[20] K. Furuno,[20] T. Gillman,[25] G. Gladding,[13] S. Gonzalez,[15] G.D. Hallewell,[27] E.L. Hart,[28] J.L. Harton,[8] A. Hasan,[4] Y. Hasegawa,[29] K. Hasuko,[29] S. J. Hedges,[3] S.S. Hertzbach,[16] M.D. Hildreth,[27] J. Huber,[20] M.E. Huffer,[27] E.W. Hughes,[27] H. Hwang,[20] Y. Iwasaki,[29] D.J. Jackson,[25] P. Jacques,[24] J. A. Jaros,[27] A.S. Johnson,[3] J.R. Johnson,[32] R.A. Johnson,[7] T. Junk,[27] R. Kajikawa,[19] M. Kalelkar,[24] H. J. Kang,[26] I. Karliner,[13] H. Kawahara,[27] H.W. Kendall,[15] Y. D. Kim,[26] M.E. King,[27] R. King,[27] R.R. Kofler,[16] N.M. Krishna,[9] R.S. Kroeger,[17] J.F. Labs,[27] M. Langston,[20] A. Lath,[15] J.A. Lauber,[9] D.W.G.S. Leith,[27] V. Lia,[15] M.X. Liu,[33] X. Liu,[6] M. Loreti,[21] A. Lu,[5] H.L. Lynch,[27] J. Ma,[31] G. Mancinelli,[22] S. Manly,[33] G. Mantovani,[22] T.W. Markiewicz,[27] T. Maruyama,[27] H. Masuda,[27] E. Mazzucato,[11] A.K. McKemey,[4] B.T. Meadows,[7] R. Messner,[27] P.M. Mockett,[31] K.C. Moffeit,[27] T.B. Moore,[33] D. Muller,[27] T. Nagamine,[27] S. Narita,[29] U. Nauenberg,[9] H. Neal,[27] M. Nussbaum,[7] Y. Ohnishi,[19] L.S. Osborne,[15] R.S. Panvini,[30] H. Park,[20] T.J. Pavel,[27] I. Peruzzi,[12][b] M. Piccolo,[12] L. Piemontese,[11] E. Pieroni,[23] K.T. Pitts,[20] R.J. Plano,[24] R. Prepost,[32] C.Y. Prescott,[27] G.D. Punkar,[27] J. Quigley,[15] B.N. Ratcliff,[27] T.W. Reeves,[30] J. Reidy,[17] P.E. Rensing,[27] L.S. Rochester,[27] P.C. Rowson,[10] J.J. Russell,[27] O.H. Saxton,[27] T. Schalk,[6] R.H. Schindler,[27] B.A. Schumm,[14] S. Sen,[33] V.V. Serbo,[32] M.H. Shaevitz,[10] J.T. Shank,[3] G. Shapiro,[14] D.J. Sherden,[27] K.D. Shmakov,[28] C. Simopoulos,[27] N.B. Sinev,[20] S.R. Smith,[27] M.B. Smy,[8] J.A. Snyder,[33] P. Stamer,[24] H. Steiner,[14] R. Steiner,[1] M.G. Strauss,[16] D. Su,[27] F. Suekane,[29] A. Sugiyama,[19] S. Suzuki,[19] M. Swartz,[27] A. Szumilo,[31] T. Takahashi,[27] F.E. Taylor,[15] E. Torrence,[15] A.I. Trandafir,[16] J.D. Turk,[33] T. Usher,[27] J. Va'vra,[27] C. Vannini,[23] E. Vella,[27] J.P. Venuti,[30] R. Verdier,[15] P.G. Verdini,[23] S.R. Wagner,[27] A.P. Waite,[27] S.J. Watts,[4] A.W. Weidemann,[28] E.R. Weiss,[31] J.S. Whitaker,[3] S.L. White,[28] F.J. Wickens,[25] D.A. Williams,[6] D.C. Williams,[15] S.H. Williams,[27] S. Willocq,[33] R.J. Wilson,[8] W.J. Wisniewski,[27] M. Woods,[27] G.B. Word,[24] J. Wyss,[21] R.K. Yamamoto,[15] J.M. Yamartino,[15] X. Yang,[20] S.J. Yellin,[5] C.C. Young,[27] H. Yuta,[29] G. Zapalac,[32] R.W. Zdarko,[27] C. Zeitlin,[20] and J. Zhou,[20]

[1]*Adelphi University, Garden City, New York 11530*
[2]*INFN Sezione di Bologna, I-40126 Bologna, Italy*
[3]*Boston University, Boston, Massachusetts 02215*
[4]*Brunel University, Uxbridge, Middlesex UB8 3PH, United Kingdom*
[5]*University of California at Santa Barbara, Santa Barbara, California 93106*
[6]*University of California at Santa Cruz, Santa Cruz, California 95064*
[7]*University of Cincinnati, Cincinnati, Ohio 45221*
[8]*Colorado State University, Fort Collins, Colorado 80523*
[9]*University of Colorado, Boulder, Colorado 80309*

$^{(10)}$ Columbia University, New York, New York 10027

$^{(11)}$ INFN Sezione di Ferrara and Università di Ferrara, I-44100 Ferrara, Italy

$^{(12)}$ INFN Lab. Nazionali di Frascati, I-00044 Frascati, Italy

$^{(13)}$ University of Illinois, Urbana, Illinois 61801

$^{(14)}$ Lawrence Berkeley Laboratory, University of California, Berkeley, California 94720

$^{(15)}$ Massachusetts Institute of Technology, Cambridge, Massachusetts 02139

$^{(16)}$ University of Massachusetts, Amherst, Massachusetts 01003

$^{(17)}$ University of Mississippi, University, Mississippi 38677

$^{(19)}$ Nagoya University, Chikusa-ku, Nagoya 464 Japan

$^{(20)}$ University of Oregon, Eugene, Oregon 97403

$^{(21)}$ INFN Sezione di Padova and Università di Padova, I-35100 Padova, Italy

$^{(22)}$ INFN Sezione di Perugia and Università di Perugia, I-06100 Perugia, Italy

$^{(23)}$ INFN Sezione di Pisa and Università di Pisa, I-56100 Pisa, Italy

$^{(24)}$ Rutgers University, Piscataway, New Jersey 08855

$^{(25)}$ Rutherford Appleton Laboratory, Chilton, Didcot, Oxon OX11 0QX United Kingdom

$^{(26)}$ Sogang University, Seoul, Korea

$^{(27)}$ Stanford Linear Accelerator Center, Stanford University, Stanford, California 94309

$^{(28)}$ University of Tennessee, Knoxville, Tennessee 37996

$^{(29)}$ Tohoku University, Sendai 980 Japan

$^{(30)}$ Vanderbilt University, Nashville, Tennessee 37235

$^{(31)}$ University of Washington, Seattle, Washington 98195

$^{(32)}$ University of Wisconsin, Madison, Wisconsin 53706

$^{(33)}$ Yale University, New Haven, Connecticut 06511

† Deceased

$^{(a)}$ Also at the Università di Genova

$^{(b)}$ Also at the Università di Perugia